Supporting Information

Horwitz et al. 10.1073/pnas.1315295110

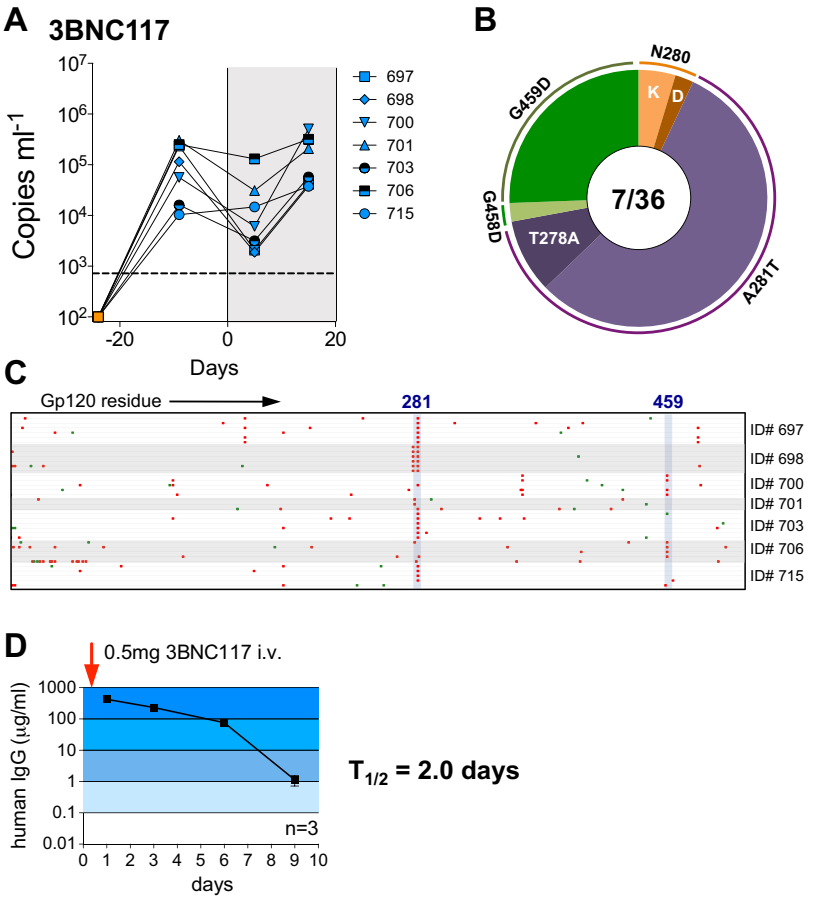

Fig. S1. Treatment of HIV-1–infected humanized mice (hu-mice) with 3BNC117 transiently reduces viral load and rapidly selects for antibody resistance mutations. (*A*) Viral loads from seven mice treated with the antibody 3BNC117 (0.5 mg twice per week s.c.). Antibody treatment began at day 0. Each line represents a single mouse. (*B* and *C*) Gp120 sequences were cloned from each mouse after 15 d of treatment with 3BNC117 (*C*). Red and green dots indicate nonsynonymous and synonymous mutations, respectively, relative to HIV-1_{YU2}. Resistance mutations were identified in the CD4 binding site (CD4bs) at residues $YU2^{(280–282)}$ and $YU2^{(458–459)}$. The representation of each mutation among the viral sequences obtained in *C* is shown in *B*, where the numbers in the center reflect the number of mice (7) and the total number of gp120 sequences obtained (36). (*D*) The serum half-life of 3BNC117 in NOD/$Rag1^{-/-}$/IL-$2R\gamma^{null}$ (NRG) mice was 2.0 d. Three NRG mice were injected with 0.5 mg 3BNC117 i.v. at day 0 and followed for 9 d. 3BNC117 concentration was measured by human IgG-specific ELISA and the half-life was calculated using GraphPad Prism 5.0.

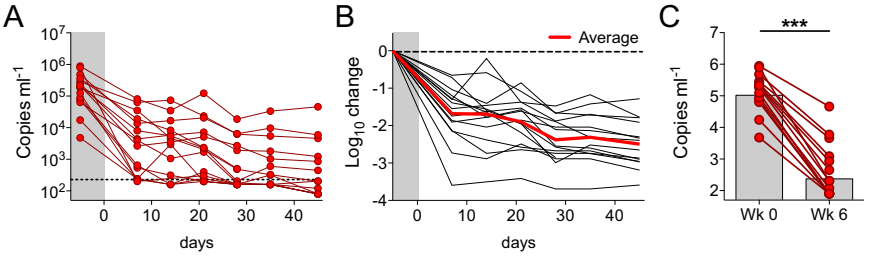

Fig. S2. Combination immunotherapy with 3BNC117, PG16, and 10-1074 is sufficient to suppress viremia in HIV-1_{YU2}–infected hu-mice. (*A*) Plasma viral loads for hu-mice treated with combination immunotherapy were monitored weekly using the highly sensitive Abbot HIV-RealTime Assay. Each line represents a single animal. Treatment began at day 0. Antibodies were administered s.c. at 1.0 mg per antibody, twice per week, for a total of 6 wk. (*B*) Fold change in viral load (shown in *A*) from the baseline measurement for each animal. Red line shows the geometric mean viral load change at each time point. (*C*) Combination immunotherapy resulted in a highly significant drop in viral load in all animals ($n = 15$) after 6 wk of continuous treatment (***$P < 0.0001$, Wilcoxon signed rank test, two-tailed). The average viral load drop was 2.5 $\log_{10}$ HIV-1 RNA copies per milliliter.

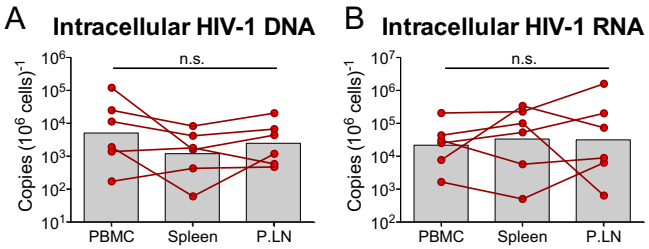

Fig. S3. Cell-associated HIV-1 DNA and RNA levels in immunotherapy-treated mice (Fig. 1) are similar among lymphoid tissue compartments. (*A* and *B*) Cell-associated HIV-1 DNA (*A*) and RNA (*B*) levels per million human lymphoid cells isolated from the indicated tissue compartment (P.LN, peripheral lymph nodes). Each line represents a single mouse. Gray bars reflect geometric averages for each tissue compartment. n.s., not statistically significant.

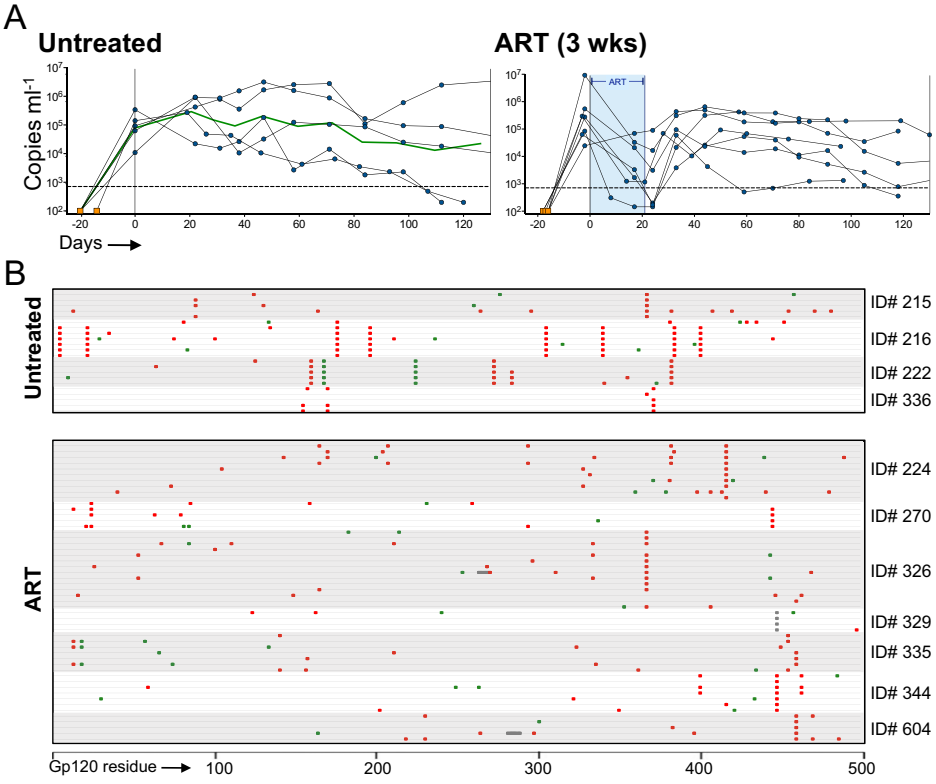

Fig. S4. Treatment of HIV-1_{YU2}–infected hu-mice with antiretroviral therapy (ART) rapidly lowers viral load, but viremia returns to pretreatment levels after stopping ART. (*A*) Untreated mice exhibit sustained viremia for over 120 d after infection (green line, geometric average). Three weeks of treatment with ART [tenofovir disproxil-fumarate/emtricitabine/raltegravir (TDF/FTC/RAL), daily by oral gavage] reduces viral load by an average of 2.0 $\log_{10}$ RNA copies per milliliter plasma. Twelve to 23 d after stopping ART, viral load returns to pretreatment levels. (*B*) gp120 sequences obtained from untreated mice (*Upper*) and ART-treated mice after stopping ART. Red and green dots indicate nonsynonymous and synonymous mutations, respectively, relative to HIV-1_{YU2}. ART-treated mice did not carry recurring mutations in gp120 that differed from those identified in untreated mice.

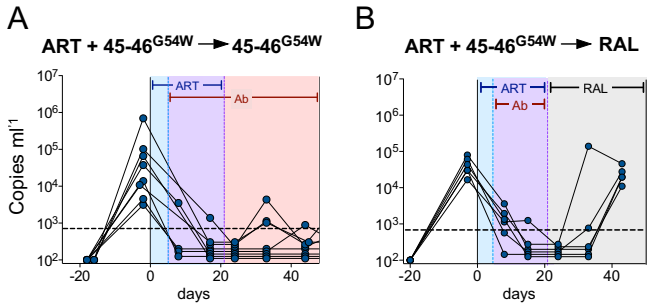

Fig. S5. Mice treated with ART plus 45-46^{G54W} combination therapy exhibit rapid viral rebound after both treatments are stopped. (*A* and *B*) Mice were treated with ART (TDF/FTC/RAL) for a total of 3 wk. Five days into ART, combination therapy was initiated with 45-46^{G54W}. Combination therapy was terminated after 3 wk on ART and mice were placed on either 45-46^{G54W} (*A*, copied from Fig. 3) or raltegravir (*B*) only. (For clarity, only mice below the limit of viral load detection at the time combination therapy was stopped are shown.) Each line represents a single mouse. In contrast to mice continuing on 45-46^{G54W} monotherapy, viremia in mice continuing on raltegravir monotherapy quickly rebounded to pretreatment levels, indicating that antibody monotherapy sustained viremic suppression after combination therapy was stopped.

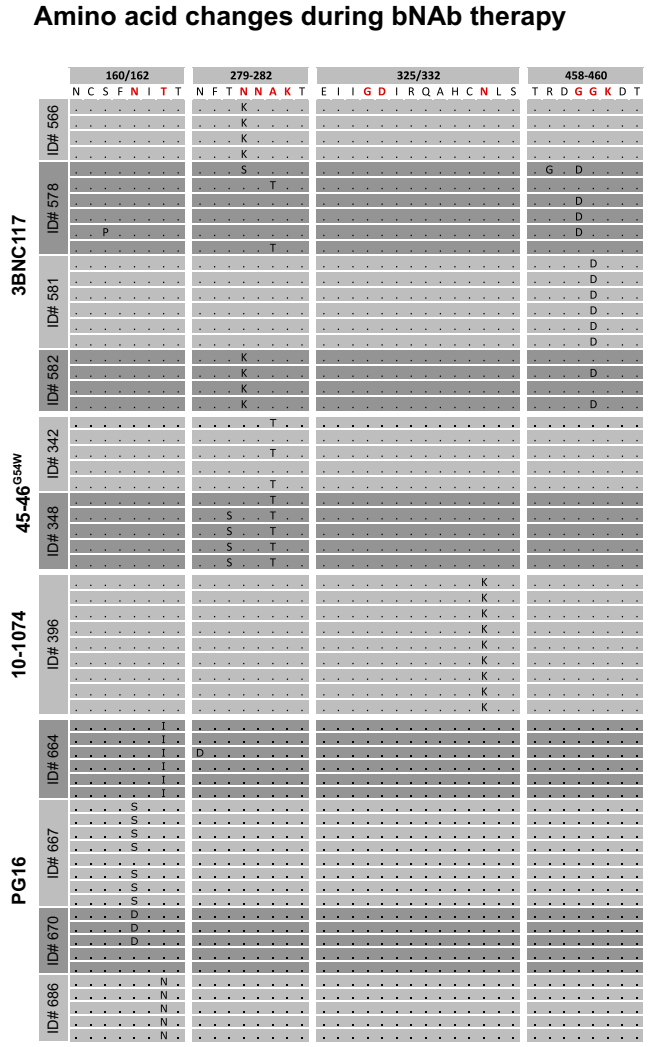

Fig. S6. Viruses in mice that escaped antibody therapy (Figs. 3 and 5*A*) harbor amino acid changes in gp120 in regions that are targeted by the antibodies (1). Amino acid changes in mice treated with either 45-46^{G54W} or 3BNC117 carried mutations at either (or both) YU2$^{(279–281)}$ or YU2$^{(458–459)}$. The one mouse escaping 10-1074 had the mutation YU2^{N332K}, and mice escaping PG16 had mutations at YU2$^{160/162}$.

1. Klein F, et al. (2012) HIV therapy by a combination of broadly neutralizing antibodies in humanized mice. *Nature* 492(7427):118–122.

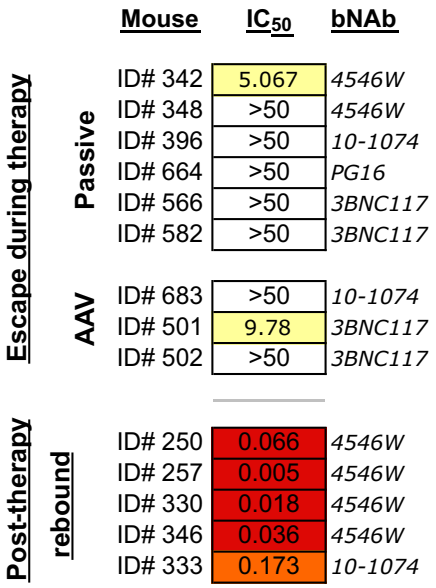

Fig. S7. Viruses emerging during antibody therapy are resistant to antibody neutralization, whereas viruses emerging after therapy remain sensitive to neutralization. Pseudoviruses expressing envelope from representative viral clones isolated from hu-mice during and after antibody therapy were assayed for neutralization in a TZM-bl assay (antibody IC_{50}s in micrograms per milliliter are shown). In all cases, viruses cloned from mice during antibody therapy were highly resistant to the respective antibody used in treatment (escape during therapy). This was true also for mice with reemergent virus during adeno-associated virus (AAV)-directed antibody therapy. By comparison, viruses cloned from mice after antibody therapy, when antibody concentrations in serum were low, remained highly sensitive to the respective antibodies used in therapy (posttherapy rebound). This suggests that reemergent virus after antibody therapy was a product of latently infected cells.

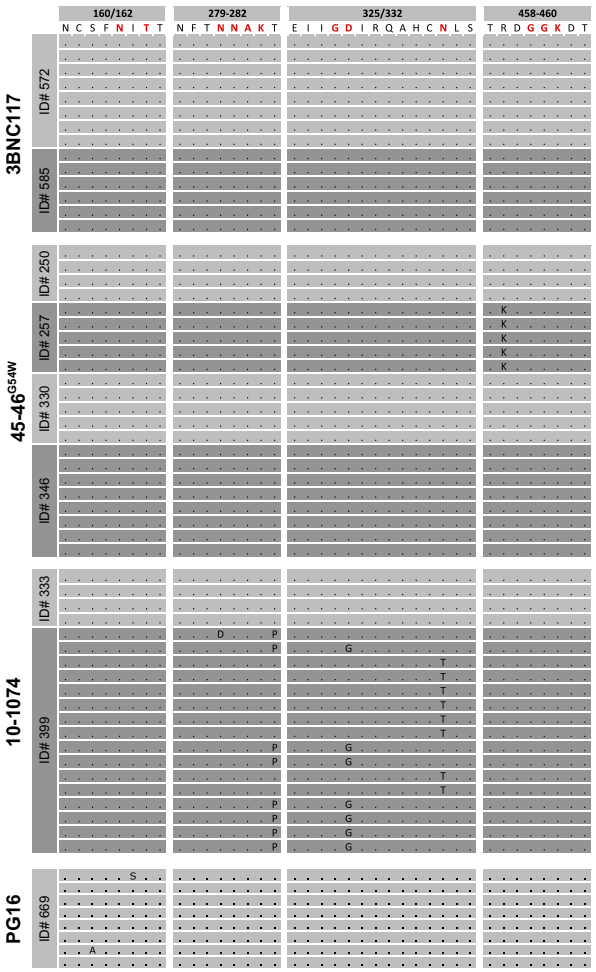

Fig. S8. Gp120 sequences from virus that rebounded after antibody concentrations in plasma decreased to subtherapeutic levels (Figs. 4 and 5*B*) generally did not harbor mutations at sites known to confer antibody resistance. Only one of nine mice for which sequences could be obtained carried mutations at resistance sites, signifying that the antibodies sustained viral suppression until rebound virus emerged from latently infected cells after antibody concentrations decayed. One 10-1074–treated mouse, ID number 399, had viral clones bearing mutations in the 10-1074 binding site at either $YU2^{D325G}$ or $YU2^{N332T}$. Of note, viremia in this mouse rebounded while antibody was still present (34 μg/mL) and this mutant virus was likely resistant to 10-1074 at this concentration.

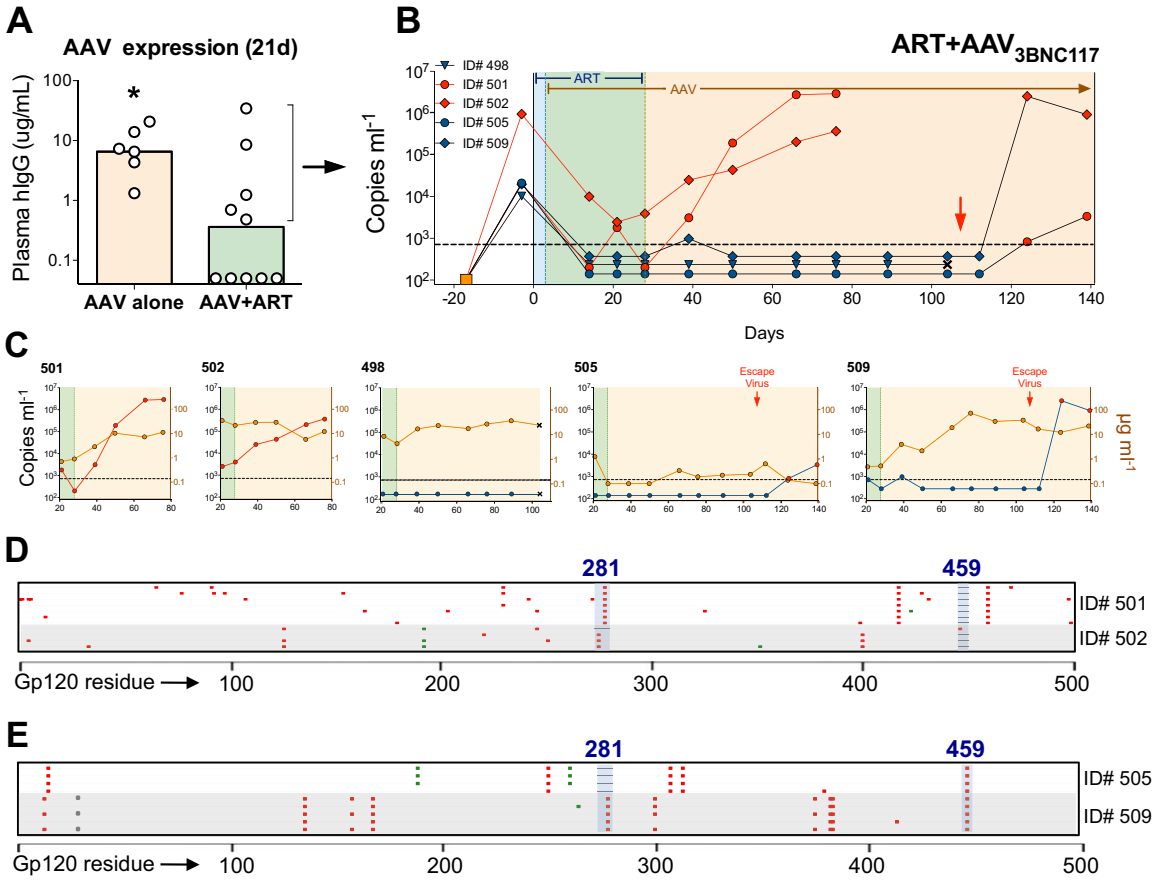

Fig. S9. Mice treated with ART and AAV-directed expression of 3BNC117 antibody exhibit sustained viral suppression after ART cessation. (*A*) Mice were injected i.v. with 2×10^{11} genomic copies of $AAV_{3BNC117}$ in the presence or absence of ART. Mice treated with ART (TDF/FTC/RAL) had significantly lower antibody expression 21 d after AAV injection ($P = 0.04$, Mann–Whitney test), possibly owing to inhibition of AAV transduction by nucleotide analogs. (*B*) The five ART plus $AAV_{3BNC117}$-treated mice with detectable antibody levels at 21 d after AAV injection (bracketed in *A*) were treated for a total of 28 d with ART. Each line represents a single mouse. ART was terminated and viral loads were monitored for an additional 80 d. Although two mice quickly escaped $AAV_{3BNC117}$ therapy upon ART termination, the remaining three mice were aviremic for more than 80 d after ART was withdrawn. The proportion of mice that remained controlled by $AAV_{3BNC117}$ was similar to results obtained for passive 3BNC117 therapy (Fig. 3). The two surviving mice at day 108 were reinfected with virus from mice that escaped 3BNC117 therapy and carried resistance mutations to that antibody. Upon reinfection virus reemerged in both mice, signifying that prolonged viral suppression was due to $AAV_{3BNC117}$ and not to loss of the human graft. (*C*) Individual viral load plots for each mouse shown in *B*, with yellow lines/symbols showing gp120-binding human IgG for each mouse. (*D* and *E*) Gp120 sequences obtained from (*D*) the two mice that escaped $AAV_{3BNC117}$ after stopping ART carried mutations conferring resistance to 3BNC117 and (*E*) virus that reemerged in $AAV_{3BNC117}$-controlled mice after reinfection at day 108 carried mutations conferring 3BNC117 resistance that were present in the reinfection inoculum. Red and green dots indicate nonsynonymous and synonymous mutations, respectively, relative to $HIV\text{-}1_{YU2}$.

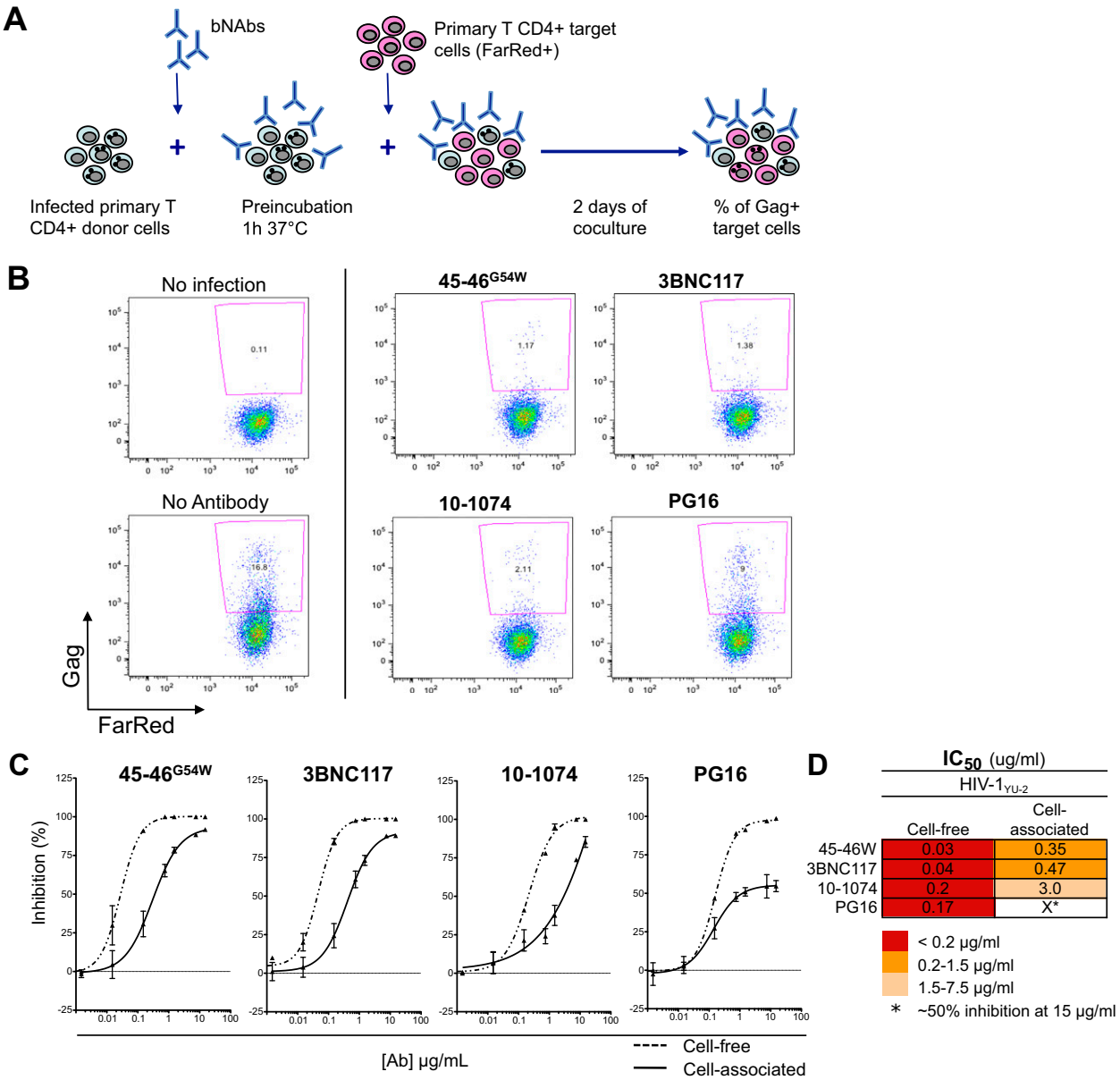

Fig. S10. Antibodies 45-46^{G54W}, 3BNC117, and 10-1074 block cell contact-mediated viral transmission in vitro. (*A*) Experimental design of an assay to measure antibody blockage of viral transmission under cell contact-permitting (cell-associated) conditions. Primary HIV-1–infected CD4+ T cells were preincubated for 1 h with broadly neutralizing antibodies (bNAbs) before coculture with autologous target cells stained with FarRed dye. After 48 h of coculture, the fraction of productively infected (Gag+) target cells was measured by flow cytometry (example shown in *B*). (*B*) Flow cytometric analysis of Gag+/FarRed+ cells after coincubation with HIV-1_{YU2}–infected donor cells (or uninfected donor cells, No infection). Donor cells were preincubated with the indicated bNAb at 15 µg/mL (or no antibody) before coincubation with FarRed+ target cells. Plots show Gag+/FarRed+ cells after 48 h of coincubation with donor cells. (*C*) Antibody-mediated inhibition of cell-free (dashed lines) and cell-associated (solid lines) viral transmission for the indicated bNAb. Cell-free infections were performed on HeLa-derived P4C5 target cells and quantitated by measuring β-gal after 36 h. Results are mean ± SD from three to five independent experiments. Curves represent fitted results. (*D*) Summary of IC_{50} values for cell-free and cell-associated viral transmission from *C*. Whereas all four antibodies potently inhibited cell-free virus transmission, 45-46^{G54W}, 3BNC117, and 10-1074 also potently inhibited viral transmission under cell contact-permitting conditions. PG16 reached only a partial IC_{50} for cell-associated viral transmission at the maximum concentration tested (15 µg/mL), possibly accounting for its reduced efficacy in vivo relative to the other bNAbs tested.